Equilibrium and Kinetics of *n*-Hexane Sorption in Pellets of 5A Zeolite

José A. C. Silva and Alírio E. Rodrigues
Laboratory of Separation and Reaction Engineering, Faculty of Engineering, University of Porto, 4099 Porto Codex, Porto, Portugal

Equilibrium, diffusion, and fixed-bed adsorption of n-hexane in pellets of 5A zeolite (Rhone–Poulenc) were studied between 373 and 573 K and at partial pressures up to 0.2 bar. Equilibrium data were obtained in a flow microbalance system. Diffusivity was studied simultaneously by gravimetric and ZLC techniques. Adsorption isotherms were satisfactorily described by a localized adsorption model developed by Nitta et al. (1984) with only one temperature-dependent parameter (coefficient of Henry's law). The isosteric heat of adsorption is 14.2 kcal/mol. Kinetic data clearly show that macropore diffusion is the controlling mass-transfer mechanism. Between 473 and 573 K, pore diffusivities range from 0.11 to 0.13 cm^2/s in the system $He-nC_6$, and from 0.06 to 0.08 cm^2/s in the system N_2-nC_6. The effect of partial pressure of sorbate, temperature, and total flow rate in the behavior of the fixed-bed unit is shown. A simple mathematical model with equilibrium and diffusivity parameters obtained in this work predicts with good accuracy all fixed-bed adsorption experiments.

Introduction

One of the first industrial adsorption processes was the separation of *n*/isoparaffins in 5A zeolite molecular sieves developed by Union Carbide in the 1960s for the octane improvement of gasoline pools and solvent production (Symoniak, 1980). Since the 1970s the development of Hysomer and the total isomerization process (TIP) by Shell and UOP, respectively, and the demand for environmental protection with the restriction of lead in fuel, makes this separation, coupled with an isomerization reactor, one of the most licensed adsorption processes in the world. The two major fractions of normal paraffins that exist in the low-range naphtha used in TIP for the improvement of the research octane numbers (RON) of gasolines are *n*-pentane and *n*-hexane (Holcombe et al., 1990; Minkinnen et al., 1993). In such processes *n*-hexane and *n*-pentane, which have low octane numbers, are partially converted to high-octane branched paraffins in an isomerization reactor. The unconverted *n*-paraffins are separated in a selective adsorption unit packed with 5A zeolite pellets and recycled to the isomerization reactor. The 5A zeolite excludes branched paraffins and adsorbs linear nC_5 and nC_6.

Correspondence concerning this article should be addressed to A. E. Rodrigues.

The successful application of zeolites as industrial adsorbents depends on the appropriate development of sorption–desorption cycles (Barrer, 1981), and this requires intensive study of phenomena such as equilibria and the kinetics of adsorption, coupled with a mathematical model that correctly describes the dynamics of fixed-bed columns. Sorption isotherms in molecular-sieve zeolites are generally type I in IUPAC classification. These isotherms can be interpreted by thermodynamic analysis using virial isotherms (e.g., Kiselev, 1971; Doetsh et al., 1974; Barrer, 1981; Ruthven and Kaul, 1996), by molecular models based on localized adsorption (e.g., Langmuir, 1918; Nitta et al., 1984; Martinez and Basmadjian, 1996), and using the potential theory (e.g., Dubinin's volume-filling theory, 1975). Zeolite molecular sieves consist of small microporous crystals formed in a macroporous pellet; kinetics of sorption in these adsorbents generally offers two distinct resistances to mass transfer: the macroporous resistance of the pellet and the microporous resistance of the crystals. Assuming these resistances in series, Ruckenstein et al. (1971) developed a bidisperse model for the measurement of transient diffusion. Based on that model, Ruthven and Loughlin (1972) proposed a simple criterion for the relative importance of time constants of diffusion. At that time most

of the measurement of transport diffusion was made by volumetric or gravimetric sorption uptake and chromatography in conjunction with the measurement of adsorption isotherms. It is well known that several transport mechanisms can be of importance in such systems, making the interpretation of kinetic data difficult (Karger and Ruthven, 1992; Hufton and Ruthven, 1993), and may lead to erroneous results. In order to minimize such effects new techniques have been developed, such as the ZLC technique of Eic and Ruthven (1988) and the thermal method of Grenier et al. (1995). With these techniques, micropore diffusion in zeolites were found to be orders of magnitude higher than data measured by gravimetry or classic chromatography. The basic concepts needed for the interpretation and modeling of fixed-bed adsorption were given by Rodrigues (1981). Equilibrium and kinetics of the sorption of paraffins up to *n*-butane in 5A zeolite pellets have been widely studied by gravimetric uptake (e.g., Youngquist et al., 1971; Ruthven and Loughlin, 1971; Ruthven and Derrah, 1972; Zuech et al., 1983); however, for paraffins with higher carbon numbers only very few data are available (e.g., Eberly, 1969; Silva and Rodrigues, 1997b).

In a previous work (Silva and Rodrigues, 1997a), equilibrium and diffusivity data of *n*-pentane in 5A zeolite pellets were reported. It was shown that the multisite-Langmuir (MSL) model of Nitta et al. (1984) predicts with good accuracy the adsorption equilibrium of *n*-pentane. Also ZLC and gravimetric studies showed that macropore diffusion is the controlling mechanism for intraparticle mass transfer. Since *n*-hexane is also a major constituent in the low-range naphtha, there is a need for a similar study.

The objectives of this work are (1) the measurement or sorption equilibrium data of nC_6 on 5A zeolite pellets by gravimetry; (2) the measurement of intraparticle diffusivity of nC_6 on 5A zeolite pellets with crystals of different sizes by ZLC and gravimetry, and (3) the prediction of breakthrough curves in a fixed-bed adsorber based on a model including parameters independently measured.

Experimental Studies

Materials and reagents

The adsorbent is extrudate 5A zeolite 1/16-in. (1.6-mm) cylindrical pellets (Rhone-Poulenc, France) $\approx$ 6 mm long. The crystals of 5A zeolite have a mean cube side of 2 μm. Mercury porosimetry studies performed in our laboratory up to a pressure of 2,000 bar are reported in Table 1. In some ZLC experiments pellets of the same size but with crystal size of 3.6 μm were also used. The *n*-hexane is 99% purity (Merck, Germany). Nitrogen and helium are type R and N50, respectively, in Air Liquide (France) classification.

Gravimetric apparatus

Equilibrium isotherms and transient desorption curves were measured gravimetrically using a C.I. Electronics (UK) flow microbalance system. Four pellets suspended in the cage were used in all experiments. The partial pressure of *n*-hexane was obtained by bubbling an inert gas (helium or nitrogen) in a wash bottle containing the liquid sorbate. The wash bottle was always immersed in a bath at subambient temperature in order to avoid condensation of paraffin on the tube walls before entering the microbalance. The maximum attainable partial pressure was restricted by the saturation vapor pressure at room temperature. Equilibrium measurements were made by increasing or decreasing the partial pressure in steps. Since significant dead volumes exist in this system, reliable kinetic data were obtained only when partial pressure was decreased from a small value to zero, since high flow rates of inert gas can be used in order to minimize the effect of dead volumes. Prior to measuring, the zeolite sample was dehydrated *in situ* by heating it from ambient temperature to 633 K in 20 mL/min pure nitrogen or helium over a period of at least 16 h. All experiments were performed at atmospheric pressure. Details of the experimental system and technique have been described elsewhere (Silva and Rodrigues, 1997).

Table 1. Mercury Porosimetry Results in Rhone–Poulenc Pellets of 5A Zeolite

Intrusion volume (cm^3/g)	0.24
Apparent density, ρ_a (g/cm^3)	1.45
Solid density, ρ_s (g/cm^3)	2.22
Porosity, ϵ_p	0.35

ZLC apparatus

The ZLC technique introduced by Eic and Ruthven (1988) for the measurement of intracrystalline diffusivity, consists of a differential bed of porous particles that is first saturated with a fluid mixture containing the adsorbable species; at time zero the carrier gas flows through the ZLC at a sufficiently high flow rate, and the desorption curve is analyzed in terms of concentration vs. time.

In our system pellets (generally 3) are placed inside a small column directly attached to a FID gas chromatograph (Carlo Erba GC 6000 Vega series, Italy). Column saturation and purging were performed by two complete separate lines in order to avoid extraneous parasitic effects such as condensation on tube walls, inaccurate definition of zero time in the system (if purge gas passes by the same saturation line, pellets in contact with the purge gas at zero time could not be made with a free sorbate gas). Sample dehydration was performed as in the gravimetric technique. Saturation of adsorbent was made with a very small partial pressure ($\approx 2\times 10^{-4}$ bar) of nC_6. Details of the experimental system and technique have been described elsewhere (Silva and Rodrigues, 1997a).

Fixed-bed apparatus

The study of adsorption and desorption of *n*-hexane was performed in a 20-cm-long stainless-steel column with a diameter of 3.35 cm. Two thermocouples were inserted axially in the column, one near the middle of the column and the other at the top. The effluent of the column was sent directly to a gas chromatograph (Carlo Erba GC 6000 Vega series, Italy) equipped with a FID detector and continuously analyzed. Before the first run the column was activated with pure nitrogen or helium by heating it from ambient temperature to 633 K with 50 mL/min (STP) for a period of at least 48 h. Details of the experimental system and technique have been described elsewhere (Silva and Rodrigues, 1997b).

Theories

Equilibrium isotherms

In a flow gravimetric system the directly measured adsorbed concentration q is a function of temperature T and the partial pressure of the sorbate p. Theories of adsorption provide explicit or implicit equations for the relations between these variables (Kiselev, 1971; Barrer, 1981; Ruthven, 1984; Yang, 1987). To obtain the values of the limiting slope of an adsorption isotherm at low pressure (or Henry's law coefficient), the selection of an isotherm model to represent experimental data should be carefully made, since several models do not conform to the rigorous definition of that limit (Talu and Myers, 1988), which is a positive and finite limiting slope. Henry's law coefficients are useful in ZLC studies or any diffusivity studies performed at low pressure, so the correctness of that parameter is very important. A suitable isotherm for a perfect gas in the gas phase at equilibrium with sorbed gas, from a thermodynamic point of view, is the virial isotherm (Kiselev, 1971; Barrer, 1981; Ruthven, 1984),

$$H = \frac{q}{p}\exp[2A_1q + (3/2)A_2q^2 + (4/3)A_3q^3 + \cdots], \quad (1)$$

where H is the Henry's law coefficient and A^{1-3} are virial coefficients. According to the virial isotherm, semilog plots of p/q vs. q extrapolated to zero concentration give us Henry's constants, which are also useful for checking the consistency of the isotherms of molecular models. The virial isotherm is suitable for interpreting data from a thermodynamic point of view, but does not give insight into sorption events at the molecular level (Barrer, 1981). The multisite Langmuir (MSL) model of Nitta et al. (1984) is a simple, analytical, flexible, as well as thermodynamically and physically consistent framework for describing pure and mixed gas adsorption from adsorbates of different sizes (Sircar, 1995). Two types of isotherms are presented by the authors for homogeneous and heterogeneous surfaces. Neglecting the interaction term between sorbed molecules, the isotherm expression for homogeneous surfaces, is

$$K_{eq} = \frac{1}{p}\frac{\theta}{(1-\theta)^n}, \quad (2)$$

where $\theta = q/q_{max}$ is the degree of filling of sites, K_{eq} is an equilibrium constant (temperature dependent), q_{max} the maximum concentration of adsorbate at the saturation of the adsorbent, and n is the number of active sites occupied by an adsorbed molecule. When n equals 1, this model leads to the Langmuir isotherm. Experimental validation of this model is simple: a plot of $\theta/p(1-\theta)^n$ against θ should be a straight line parallel to the θ axis, with intercept at zero loading, which gives the equilibrium constant, which in turn, multiplied by q_{max}, gives the Henry's law coefficient H.

Kinetics of sorption

In bidisperse porous adsorbents such as zeolite pellets there are two diffusion mechanisms: the macropore diffusion with time constant R_p^2/D_p and the micropore diffusion with time constant r_c^2/D_c. Assuming that the diffusion mechanisms are in series, Ruckenstein et al. (1971) developed a bidisperse porous model applied to the measurement of transient diffusion in systems with linear isotherm. Based on this model Ruthven and Loughlin (1972) developed a criterion for the relative importance of the diffusion mechanisms, which is given by γ:

$$\gamma = \frac{(D_c/r_c^2)(1+K)}{D_p/R_p^2} \quad (3)$$

where $K = (1-\epsilon_p)H_{ad}/\epsilon_p$ is the capacity factor and H_{ad} ($= \rho_s RTH/M_w$) is the dimensionless Henry's constant or local slope of the isotherm. Macropore diffusivity is the controlling mechanism for $\gamma > 10$; crystal diffusivity is the controlling mechanism for $\gamma < 0.1$; if $0.1 < \gamma < 10$, both macropore and crystal diffusivity should be taken into account.

Bidisperse porous models for ZLC desorption curves have recently been developed by Brandani (1996) and Silva and Rodrigues (1996). A relevant solution for a ZLC model in a macropore diffusion-controlled system considering pellets as an infinite cylinder is (Crank, 1975),

$$\frac{C_{out}}{C_0} = 2L\sum_{n=1}^{\infty}\frac{\exp\left[-\beta_n^2 D_p t/R_p^2(1+K)\right]}{(\beta_n^2 + L^2)}, \quad (4)$$

where

$$\beta_n J_1(\beta_n) - LJ_0(\beta_n) = 0 \quad (5)$$

$$L = \frac{1}{2}\frac{\text{Purge flow rate}}{\text{Pellets volume}}\frac{R_p^2}{\epsilon_p D_p}, \quad (6)$$

where C_{out} is the outlet concentration of the ZLC cell; C_0 is the concentration at time zero in the ZLC cell; β_n are roots of transcendental Eq. 5; $J_1(\beta_n)$ and $J_0(\beta_n)$ are Bessel functions of the first kind.

According to Eic and Ruthven (1988), an easy way to determine model parameters is to use the information of desorption curves at long times. Model series represented in Eq. 4 at long times reduces to

$$\ln\left(\frac{C_{out}}{C_0}\right) = \ln\left(\frac{2L}{\beta_1^2 + L^2}\right) - \frac{\beta_1^2 D_p t}{R_p^2(1+K)}. \quad (7)$$

Using intercept and slope information in experimental curves in conjunction with the definition of parameter L, the relevant equations to obtain model parameters are

$$\frac{2L}{\beta_1^2 + L^2} = \text{Intercept}; \qquad -\frac{\beta_1^2 D_p}{R_p^2(1+K)} = \text{Slope};$$

$$L\frac{\epsilon_p D_p}{R_p^2} = \frac{1}{2}\frac{\text{Purge flow rate}}{\text{Pellets volume}},$$

where Intercept and Slope are experimental information. Another way was to use the experimental vaues of the intercept and slope represented in Eq. 7 and the transcendental Eq. 5. The two methods should give the same parameters.

In a flow gravimetric system the experiments are similar to the ZLC ones except that the measured variable is not the outlet concentration of the ZLC but the amount of sorbate leaving the pellet at a certain time. Assuming that heat effects can be neglected and differential steps in pressure are used, the solution of the model is (Crank, 1975)

$$\frac{M_t}{M_0} = 4L^2 \sum_{n=1}^{\infty} \frac{\exp\left[-\beta_n^2 D_p t/R_p^2(1+K)\right]}{\beta_n^2(\beta_n^2 + L^2)}, \qquad (8)$$

where M_t is the amount of sorbate in the pellet at time t, and M_0 is the amount of sorbate in the pellet at time zero. If $L \to \infty$, then Eq. 8 reduces to (Crank, 1975)

$$\frac{M_t}{M_0} = 4 \sum_{n=1}^{\infty} \frac{1}{\beta_n^2} \exp\left[-\beta_n^2 D_p t/R_p^2(1+K)\right], \qquad (9)$$

where β_n are calculated from $J_0(\beta_n) = 0$. For more than 70% uptake only the first term is relevant, and the model reduces to

$$\ln\left(\frac{M_t}{M_0}\right) = \ln\left(\frac{4}{\beta_1^2}\right) - \frac{\beta_1^2 D_p t}{R_p^2(1+K)}. \qquad (10)$$

In order to apply Eq. 10, experimental data of M_t/M_0 vs. time t in a semilog plot should be a straight line at long times with slope $-\beta_1^2 D_p/R_p^2(1+K)$ and intercept $4/\beta_1^2$.

It should be stressed that when dealing with Eqs. 7 or 10 the parameter K defined by $(1-\epsilon_p)H_{ad}/\epsilon_p$ should be independently measured from isotherms.

Fixed-bed adsorption

In order to study the adsorption behavior of *n*-hexane in a fixed-bed, a dynamic model was developed. The adsorption system considered is a nonisothermal, nonadiabatic column packed with pellets of 5A zeolite, through which an inert gas flows in steady state. At time zero, the sorbate and an inert gas are introduced at the bottom of column. The mixture is fed until the column is saturated; then a cocurrent or countercurrent purge of the column with inert gas is carried out. The following additional assumptions are made:

1. Ideal gas is used.
2. The total pressure is constant during sorption process.
3. The flow pattern is described by the axial dispersed-plug flow model.
4. The main resistances to mass transfer are external fluid-film resistance and macropore diffusion in series. External film resistances and macropore diffusion can be combined in a global resistance according to a lumped model for the adsorbent particle, as suggested by Morbidelli et al. (1982).
5. A resistance to heat transfer exists in the external fluid film around the solid.
6. The temperature dependence of gas and solid properties are neglected.
7. The adsorption equilibrium is described by Nitta et al.'s isotherm according to data contained in that article.

Table 2. Mathematical Model for Study of Fixed-Bed Adsorption

Overall mass balance

$$\frac{\partial F}{\partial z} + \epsilon_b \frac{\partial \rho}{\partial t} + (1-\epsilon_b)\rho_a \frac{\partial \langle q \rangle}{\partial t} = 0$$

Mass balance to sorbate species

$$\epsilon_b D_L \frac{\partial}{\partial z}\left(\rho \frac{\partial y_a}{\partial z}\right) = \frac{\partial}{\partial z}(F y_a) + \epsilon_b \frac{\partial}{\partial t}(\rho y_a) + (1-\epsilon_b)\rho_a \frac{\partial \langle q \rangle}{\partial t}$$

Mass-transfer rate to solid

$$\rho_a \frac{\partial \langle q \rangle}{\partial t} = a_p K_{gl} \rho (y_a - \langle y_a \rangle)$$

Energy balance (gas phase)

$$K_L \frac{\partial^2 T}{\partial z^2} = FC_{pg} \frac{\partial T}{\partial z} + \epsilon_b \rho C_{pg} \frac{\partial T}{\partial t} + (1-\epsilon_b) a_p h_p (T - T_s) + a_c h_w (T - T_w)$$

Energy balance (solid phase)

$$\rho_s C_{ps} \frac{\partial T_s}{\partial t} = a_p h_p (T - T_s) + (-q_{st})\rho_a \frac{\partial \langle q \rangle}{\partial t}$$

Model equations are presented in Table 2. Danckwerts boundary conditions are used for the mass balance of sorbate species and the energy balance of the gas phase. The model equations were numerically solved by orthogonal collocation (Villadsen and Michelsen, 1978). Details of the description and a numerical solution of the model can be found elsewhere (Silva and Rodrigues, 1997b).

Results and Discussion

Adsorption equilibrium isotherms

Figure 1 shows *n*-hexane experimental adsorption equilibrium isotherms on 5A zeolite pellets. The isosteric heat of adsorption q_{st} vs. sorbate concentration q is shown in Figure 2. The values of q_{st} were calculated by

$$q_{st} = RT^2 \left(\frac{\partial \ln p}{\partial T}\right)_q, \qquad (11)$$

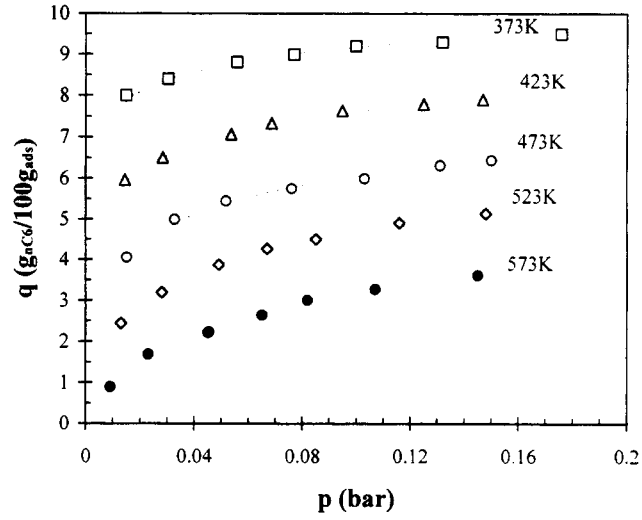

Figure 1. Adsorption equilibrium isotherms of *n*-hexane in pellets of 5A zeolite.

Points are experimental results; lines are calculated isotherms from the Nitta et al. model. Absolute temperatures are quoted in each curve.

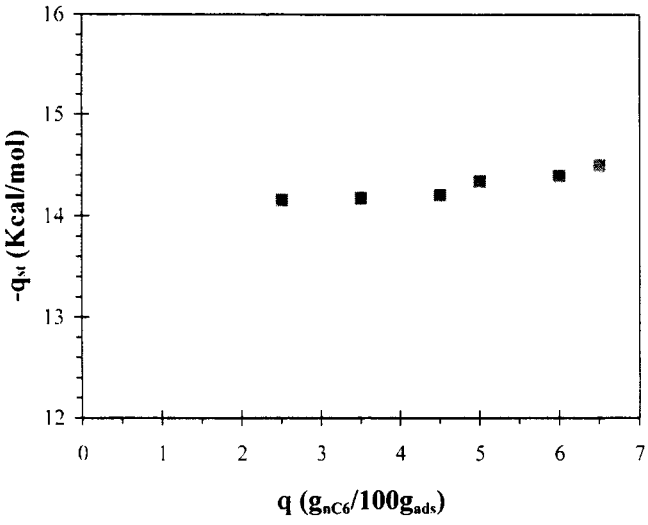

Figure 2. Isosteric heats of adsorption $-q_{st}$ as a function of adsorbed phase concentration q.

where T is the absolute temperature, p is the partial pressure of sorbate, and q is the concentration of sorbate in the adsorbed phase. The isosteric heat of adsorption is around 14.2 kcal/mol similar to the value obtained by Ruthven and Kaul (1996) for sorption of n-hexane in zeolite NaX. According to virial isotherm, Figure 3 shows semilog plots of p/q vs. q for the experimental isotherms. Extrapolation to zero loading is possible in the temperature range, 523–573 K but not at lower temperatures, because high adsorbent loading at small partial pressure of sorbate makes extrapolation difficult. Table 3 summarizes Henry's coefficients obtained from extrapolation of data plotted in Figure 3 to zero concentration. Values of q_{st}, according to a Van't Hoff dependency of Henry's constants with temperature [$H = k_0 \exp(-q_{st}/RT)$], are also shown in Table 3.

From the analysis of Nitta et al.'s isotherm it is necessary to measure q_{max}; unfortunately, this is not experimentally feasible. For the adsorption of n-pentane it has been shown

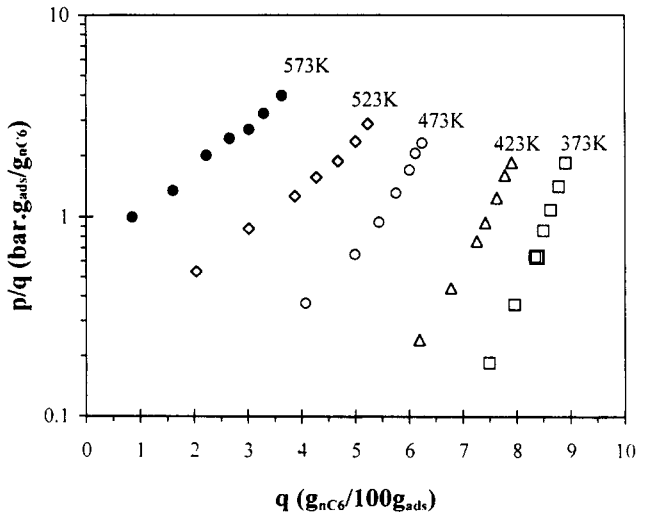

Figure 3. Semilog plot of p/q vs. q for analysis of virial isotherm.

Table 3. Henry's Coefficients and Isosteric Heats of Adsorption Calculated from Virial Isotherm and Nitta et al. Model According to Experimental Data of this Work

Temp. K	Virial Isot., H g/g·bar	Nitta et al. Isot., H g/g·bar
573	1.54	1.67
523	5	6.76
473	—	26
423	—	152
373	—	1436
$-q_{st}$ (kcal/mol)	14.0	14.2

(Silva and Rodrigues, 1997a) that $q_{max} = 13g/100g_{ads}$ is an acceptable value. To maintain thermodynamic consistency, Nitta et al.'s isotherm requires that,

$$n \cdot q_{max}/M_w = \text{const.}$$

Since $n = 5$ and $q_{max} = 13g/100g_{ads}$ with n-pentane in this work, n should be 6. Figure 4 shows a plot of $\theta/p(1-\theta)^6$ against θ, and Figure 1 shows Nitta et al.'s model superimposed on the experimental data. Henry's coefficients, obtained by the intercept at zero loading in Figure 4, are shown in Table 3; they range from 1.67 to 1436 g_{nC_6}/g_{ads} bar between 573 and 373 K, respectively. Figures 1 and 4 clearly show that results predicted by the Nitta et al. model are in good agreement with the experimental data. All parameters calculated in a straightforward way have physical meaning, and only the Henry's coefficient is temperature dependent. The parameters obtained are also in conformity with the ones obtained for n-pentane. The model of Nitta et al. (1984) can be extended to multicomponent systems and predict azeotropes, as pointed out by Sircar (1995) and Martinez and Basmadjian (1996), so it will be tested in multicomponent systems in future work.

Kinetics of sorption

For this system an estimate of the relative importance of diffusional resistances can be made. For example, at 573 K

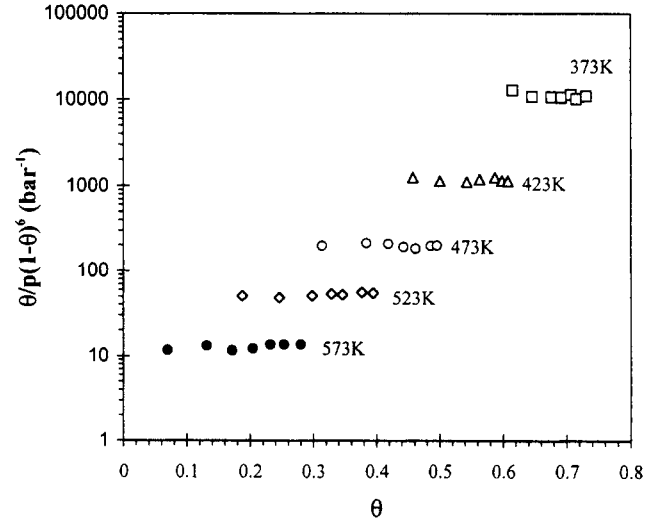

Figure 4. Semilog plot of $\theta/p(1-\theta)^6$ vs. θ for adsorption of n-hexane in pellets of 5A zeolite.

$D_{m(He-nC_6)} \approx 0.95$ cm^2/s; assuming tortuosity $T_p = 4$ and particle porosity $\epsilon_p = 0.35$ as common values in a zeolite pellet, the capacity factor K calculated in the linear region of the isotherm is $K = 3{,}823$; for a pellet with radius $R_p = 0.08$ cm, the apparent time constant for diffusion in macropores will be $D_p/R_p^2(1+K) = 0.0097\ s^{-1}$. For micropore diffusion in the work of Cavalcante et al. (1995), a value of $D_c \approx 1 \times 10^{-8}$ cm^2/s at 573 K is shown for a nC_6 paraffin in 5A zeolite, from which we calculate $D_c/r_c^2 \approx 1\ s^{-1}$ and $\gamma = 103$, which suggests a macropore diffusion-controlled regime.

In bidisperse porous adsorbents, it is important to carry out experiments in pellets with different sizes but with the same crystal size (different R_p, same r_c) or pellets with the same size but with different crystal size (same R_p, different r_c). If macropore diffusion is dominant, time constants for diffusion should depend directly on pellet size and should be insensitive to crystal size changes. If micropore diffusion controls, the reverse is true. The influence of temperature is also important: when macropore diffusion is dominant, the apparent time constant of diffusion defined by $D_p/R_p^2(1+K)$ is temperature dependent in the same order of K, which is determined independently from the isotherm. The type of purge gas is also important: if micropore diffusion is dominant, gravimetric and ZLC desorption curves should be independent of the kind of purge gas. To test the consistency of the ZLC and gravimetric model, it is important to perform experiments with different purge-gas flow rates: all diffusion parameters should be the same at a given temperature.

Effect of Purge Gas and Purge-Gas Flow Rate on ZLC Desorption Curves. Figures 5a and 5b show the effect of purge-gas flow rate on the desorption curves at 573 K, obtained by the ZLC technique for the N_2-nC_6 and $He-nC_6$ systems, respectively. It is apparent from the figure that the desorption curves are sensitive to the nature of the purge gas; desorption in the $He-nC_6$ system is faster than in the N_2-nC_6 system. This is an indication that micropore diffusion is not the total resistance in the system, but no information concerning the controlling mechanism can be drawn.

Effect of Crystal Size on ZLC Desorption Curves. The effect of crystal size on the desorption curves in the $He-nC_6$ system is shown in Figure 6; experiments are carried out with the same pellet size. Desorption curves are insensitive to variations in crystal size, so it is clear that the controlling resistance to mass transfer is the macropore diffusion.

Effect of Temperature in ZLC Desorption Curves. The effect of temperature on desorption curves for the $He-nC_6$ system is shown in Figure 7, revealing a strong temperature dependence of desorption time (which can be erroneously interpreted as an activated diffusion with activation energy on the order of the heat of adsorption), clearly indicating macropore diffusion control.

According to these results, a model for ZLC desorption curves, taking into account only macropore diffusion, is the relevant one. Model parameters calculated by the procedure described previously are summarized in Table 4 for the $He-nC_6$ and N_2-nC_6 systems at temperatures of 473 K to 573 K. Time constants of diffusion are weakly temperature dependent, which is consistent with macropore diffusion control; however, apparent time constants for diffusion defined

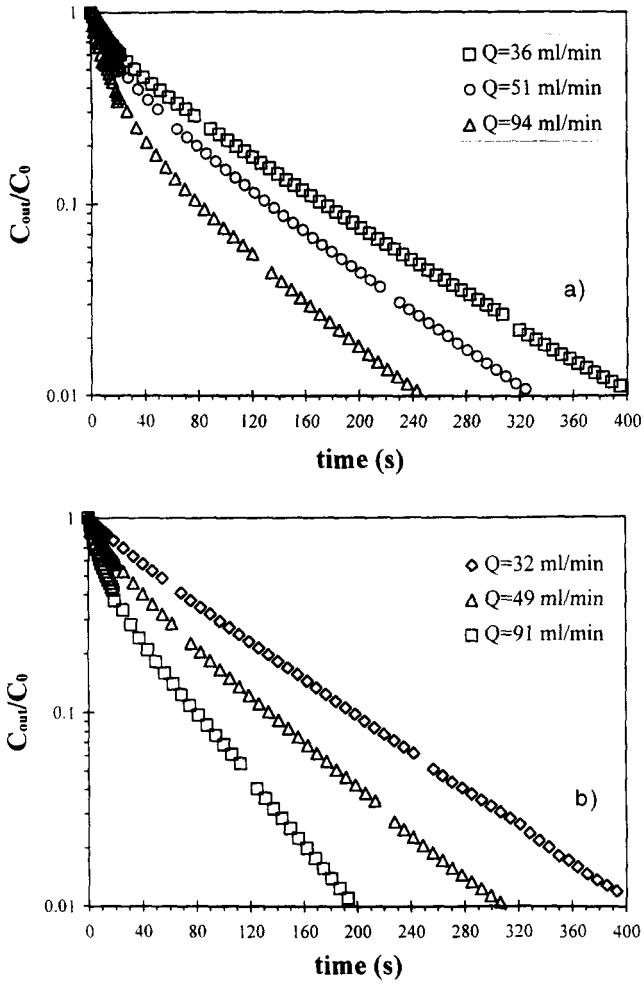

Figure 5. Effect of purge flow rate and purge gas in semilog plots of C_{out}/C_0 vs. t obtained in the ZLC system.

(a) N_2-nC_6 at 573 K; (b) $He-nC_6$ at 573 K.

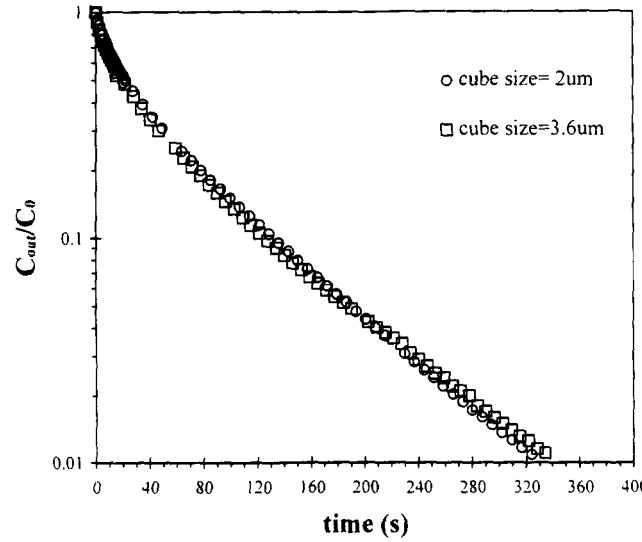

Figure 6. Effect of crystal size on pellets at 573 K in the system $He-nC_6$: semilog plot of C_{out}/C_0 vs. time t in the ZLC system.

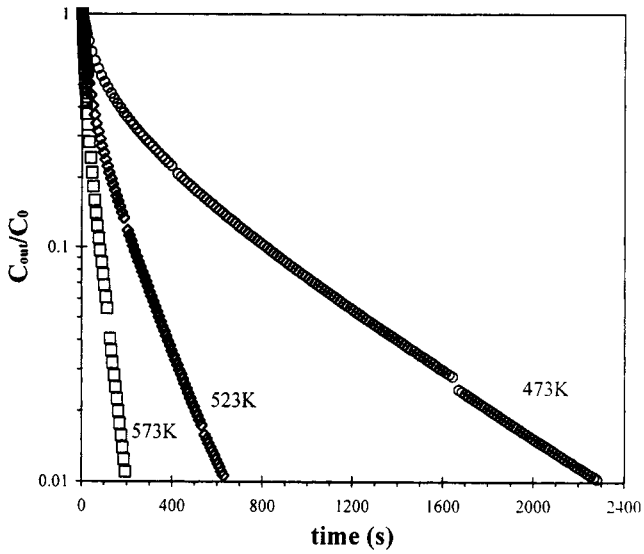

Figure 7. Effect of temperature on desorption curves in the system He–nC_6: semilog plot of C_{out}/C_0 vs. time t in the ZLC system; absolute temperatures are quoted in each curve.

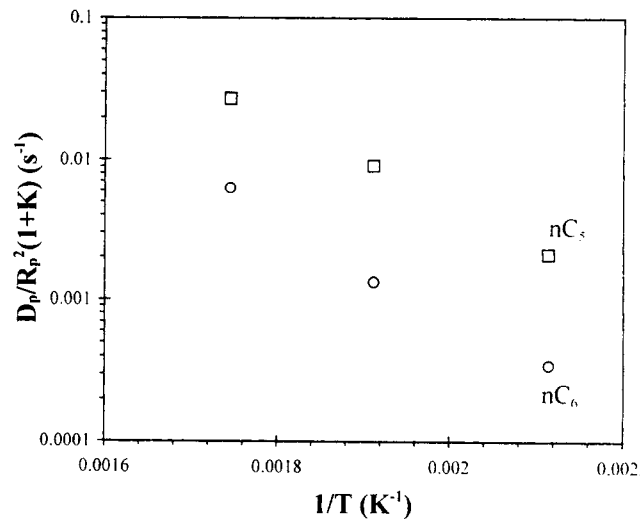

Figure 8. Apparent time constant for diffusion $D_p/R_p^2(1+K)$ vs. $1/T$ for the system He–nC_6 obtained by the ZLC technique.

by $D_p/R_p^2(1+K)$ plotted vs. $1/T$ in Figure 8 for the He–nC_6 system, are strongly temperature dependent with an activation energy of 14.6 kcal/mol, which is of the order of heat of adsorption of 14.2 kcal/mol. Time constants range from 0.00035 s^{-1} at 473 K up to 0.0053 s^{-1} at 573 K. In Figure 8 we also plot data obtained for *n*-pentane (Silva and Rodrigues, 1997a) at the same experimental conditions.

Table 4. Experimental Conditions and Model Results of Diffusion Parameters in the ZLC Technique

Q mL/min	Intercept	Slope s^{-1}	τ_{dif} (s)	L	β_1
System N_2–nC_6					
		Temperature 573 K			
36	0.60	0.0092	0.21	2.1	1.61
51	0.47	0.011	0.23	3.2	1.82
94	0.30	0.014	0.22	6.0	2.06
			Avg. 0.22		
		Temperature 523 K			
63	0.37	0.003	0.26	4.6	1.96
		Temperature 473 K			
111	0.20	0.00087	0.31	9.5	2.14
System He-nC_6					
		Temperature 573 K			
32	0.81	0.010	0.112	1.0	1.23
49	0.60	0.013	0.151	2.1	1.62
91	0.42	0.018	0.150	3.8	1.90
			Avg. 0.14		
		Temperature 523 K			
55	0.56	0.0039	0.151	2.3	1.70
76	0.50	0.0047	0.138	2.9	1.77
117	0.35	0.0057	0.148	4.9	2.04
			Avg. 0.15		
		Temperature 473 K			
122	0.32	0.0015	0.16	5.5	2.05

In order to check if the gravimetric technique leads to similar results obtained by ZLC, gravimetric experiments were performed under similar conditions to the ZLC. The adsorbent was saturated with a small partial pressure of paraffin ($\approx 2\times10^{-4}$ bar), in order to ensure the validity of Henry's law, and desorbed with a high purge-gas flow rate (near 600 mL/min STP). Figure 9 shows the effect of temperature on the desorption curves obtained with a high purge-gas flow rate of helium in order to guarantee a high value of L to validate Eq. 10. Desorption curves are well described by the theory outlined previously. The apparent time constants of

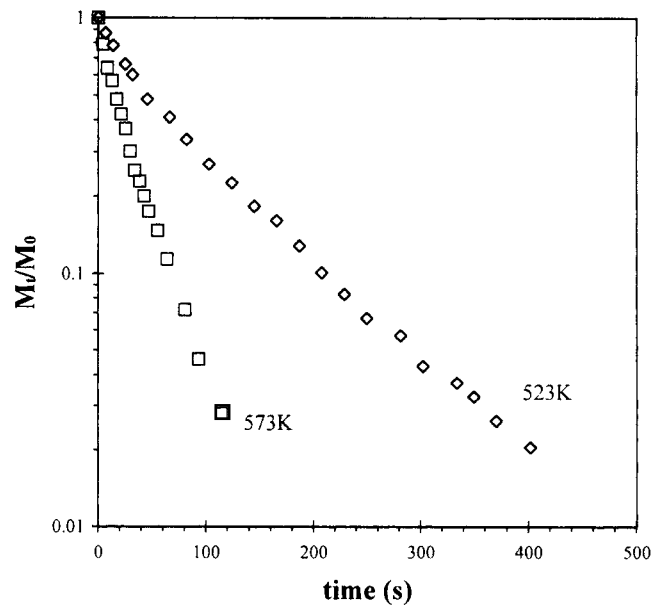

Figure 9. Effect of temperature in uptake desorption curves in the system He–nC_6 obtained by the gravimetric technique; absolute temperatures are quoted in each curve.

Table 5. Experimental Pore Diffusivities of *n*-Hexane on 5A Zeolite Pellets and Tortuosities

Temp. K	τ_{dif} s	$D_{p,exp}$ cm²/s	D_m cm²/s	D_k cm²/s	T_p
System N_2-nC_6					
573	0.22	0.08	0.25	0.25	1.6
523	0.26	0.07	0.21	0.24	1.6
473	0.31	0.06	0.18	0.23	1.7
System $He-nC_6$					
573	0.14	0.13	0.95	0.25	1.5
523	0.15	0.12	0.82	0.24	1.5
473	0.16	0.11	0.69	0.23	1.6

diffusion $D_p/R_p^2(1+K)$ calculated from the long time slopes in Figure 9 ranged from 0.00086 s^{-1} at 523 K to 0.0028 s^{-1} at 573 K. Both techniques gave the same temperature dependence in apparent time constants of diffusion; however, the values obtained by gravimetry are smaller than those obtained by the ZLC technique. The results obtained by gravimetric and ZLC techniques show that at low adsorbent loading, the macropore diffusion time constant controls the mass transfer in the $He-nC_6$ and N_2-nC_6 systems.

Diffusion mechanisms in macropores are Knudsen diffusivity in series with molecular diffusion, and so the pore diffusivity is

$$D_p = \frac{1}{T_p\left\{\frac{1}{D_m}+\frac{1}{D_K}\right\}}. \qquad (12)$$

In Table 5 we summarize the values of experimental pore diffusivity D_p (obtained from values of $\tau_{dif} = R_p^2/\epsilon_p D_p$ shown in Table 4), Knudsen diffusivity D_K [average pore radius of 0.17 μm as in Rodrigues et al. (1996)], molecular diffusivity D_m (estimated by the Chapman–Enskog equation), and tortuosity factors T_p predicted by Eq. 12. The values of T_p are similar in both systems and do not change with temperature, suggesting that Eq. 12 represents with good accuracy the macropore diffusion mechanisms of these systems.

Fixed-bed adsorption

Experimental adsorption and desorption runs were performed in order to study the influence of temperature, adsorbate partial pressure, and flow rate on the performance of the adsorption unit. At the same time validation of the model was tested relative to experiments made with equilibrium and diffusion data obtained in this work. In Table 6 the experimental conditions and model parameters used in the following study are summarized.

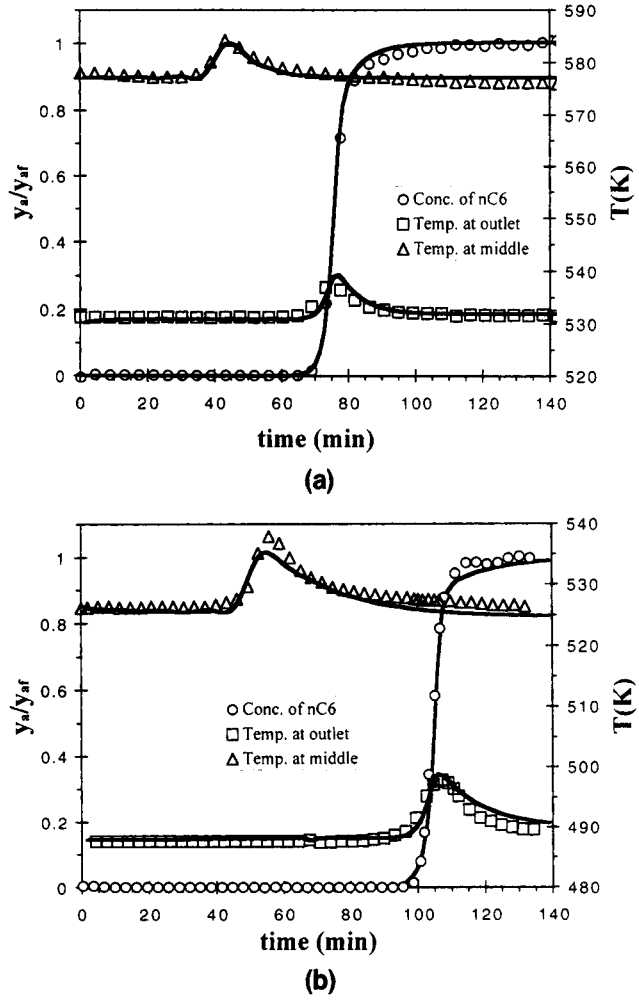

Figure 10. Effect of feed temperature on experimental breakthrough curves of *n*-hexane, temperature histories at bed exit, and temperature profiles at 10 cm from bed inlet for adsorption of a mixture of N_2-nC_6 in pellets of zeolite 5A.

(a) T_f = 513 K; y_{af} = 0.103; Q = 161 mL/min (STP); P_0 = 1 atm. (b) T_f = 469 K; y_{af} = 0.103; Q = 155 mL/min (STP); P_0 = 1 atm. The lines are theoretical curves calculated according to the numerical solution of the dynamic model with parameters given in Table 6.

Effect of Temperature. Figures 10a and 10b show the effect of temperature in adsorption breakthrough curves for bed

Table 6. Experimental Conditions and Model Parameters for Fixed-Bed Experiments

		Experimental Conditions			Model Parameters				
Runs	Figs.	F mol/m²·s	T_f K	y_{af}	$D_{L\times10^5}$ m²/s	K_L W/m·K	$K_{g\times10^2}$ m/s	h_p W/m²·K	h_w W/m²·K
11	11b, 12b	0.124	513	0.028	9.0	0.32	0.84	6.8	13.7
12	12a, 13	0.341	513	0.028	24.1	0.33	0.87	7.7	15.8
13	10a, 11a	0.124	513	0.103	7.5	0.32	0.83	6.9	13.2
21	10b	0.120	469	0.103	6.6	0.32	0.87	6.3	13.1
31	13	0.341	513	0.00	24.1	0.33	0.87	7.7	15.8
32	13	0.471	513	0.00	35.2	0.35	0.89	8.2	16.8

inlet temperatures of 513 K and 469 K, respectively. The total flow rate (160 mL/min at STP), partial pressure of n-hexane ($y_{af} = 0.028$), and total pressure ($P_0 = 1$ atm) were kept constant during the experiments. The time evolution of the bed temperature at the column outlet and at the middle of the column is also shown. Here we note that a significant difference in the temperature at the column's middle and at the fixed-bed outlet exists at the beginning of the experiments, as can be seen in Figure 10. This is due to a parabolic profile existing in the oven. The maximum temperature is located at the middle of the oven, and decreases to both ends. Since the fixed bed occupies all the oven, this effect reflects in a nonuniform temperature in the adsorber similar to that found in the oven. This profile is fixed and independent of adsorption in the fixed bed. Breakthrough curves are rather sharp, which is expected since the isotherm of n-hexane is highly favorable at the partial pressure studied, and the global mass transfer coefficient is quite high ($a_p K_{g1} = 24\ s^{-1}$ at 513 K to $a_p K_{g1} = 22\ s^{-1}$ at 469 K). The adsorbed concentration increases when temperature decreases as a consequence of the high heat of adsorption of n-hexane of 14.2 kcal/mol predicted by Nitta et al.'s isotherm. As the temperature decreases, more heat is generated during sorption, as we can see from the evolution of the temperature at the column's outlet; the temperature increases about 7 K at 513 K and 15 K at 496 K. The final approach of the breakthrough curve to the equilibrium value is slow as a consequence of the temperature increase owed to adsorption; only when the temperature reaches its equilibrium value does the breakthrough curve reach the feed composition. Model predictions are in close agreement with the experimental results, as shown in Figure 10. The values of the parameters concerning heat transfer at the wall and from solid to bulk fluid, which are determined in order to match the experimental curves, ranged from 13.1 W/m^2·K to 16.8 W/m^2·K, and from 6.8 W/m^2·K to 8.2 W/m^2·K, respectively.

Effect of Partial Pressure of n-Hexane in the Feed. The effect of n-hexane partial pressure on the feed at $T_f = 513$ K and constant feed flow rate (161 mL/min STP) is shown in Figures 11a and 11b for partial pressures $y_{af} = 0.103$ and $y_{af} = 0.028$. The adsorbent capacity decreases at lower nC_6 partial pressure; breakthrough curves are sharper when the partial pressure of nC_6 increases. The stoichiometric time decreases when nC_6 partial pressure increases as a consequence of the favorable nature of the adsorption equilibrium isotherm. In fact, a simple global mass balance over the adsorption column leads to $t_{st} = (L/v_i)[1 + (1 - \epsilon_b)\rho_a q_{af}/\epsilon_b y_{af} \rho]$. Sharper profiles with increasing partial pressures are observed and are a consequence of favorable isotherms that have origins in compressive waves, according to the equilibrium theory. The sharper breakthrough curve is also a consequence of velocity changes due to adsorption, as pointed out by Yang (1987). The same information is obtained from temperature data: higher partial pressures lead to higher, narrow peaks; in contrast, lower partial pressures lead to smaller, wider peaks. Model results are also shown in Figures 11a and 11b, predicting with good accuracy the observed adsorber behavior.

Effect of Total Flow Rate. Figures 12a and 12b show the influence of the total flow rate on the breakthrough curves at 513 K and $y_{af} = 0.028$ for total flow rate 441 and 161 mL/min

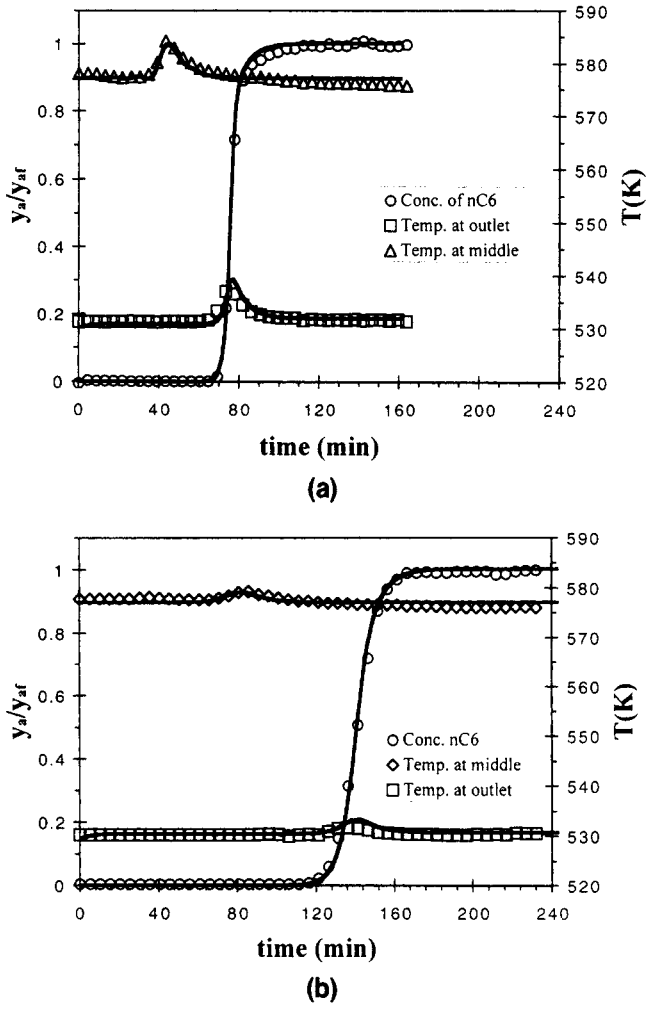

Figure 11. Effect of partial pressure of n-hexane on experimental breakthrough curves, temperature histories at bed exit, and at 10 cm from bed inlet for adsorption of a mixture of N_2–nC_6 in pellets of zeolite 5A.

(a) $T_f = 513$ K; $y_{af} = 0.103$; $Q = 161$ mL/min (STP); $P_0 = 1$ atm. (b) $T_f = 513$ K; $y_{af} = 0.028$; $Q = 161$ mL/min (STP); $P_0 = 1$ atm. The lines are theoretical curves calculated according to the numerical solution of the dynamic model with parameters given in Table 6.

STP, respectively. The total flow rate practically does not affect the shape of the breakthrough curves, which is an indication that axial and heat mass-dispersion coefficients are not limiting phenomena in the system. This analysis can be clearly seen if we normalize the real time by the respective stoichiometric time; similar breakthrough curves are then obtained. Clearly breakthrough curves occur faster at higher flow rates, as can be deduced from the relation $t_{st} = (L/v_i)[1 + (1 - \epsilon_b)\rho_a q_{af}/\epsilon_b y_{af} \rho]$. The proportionality between stoichiometric time and flow rate indicates that constant pattern conditions are valid. Again model predictions are in good agreement with experimental data, relative to concentration and temperature evolution.

Effect of Purge-Gas Flow Rate in Desorption Curves. Figure 13 shows the effect of purge-gas flow rate on the desorption of a bed saturated with n-hexane at a partial pressure of 0.028

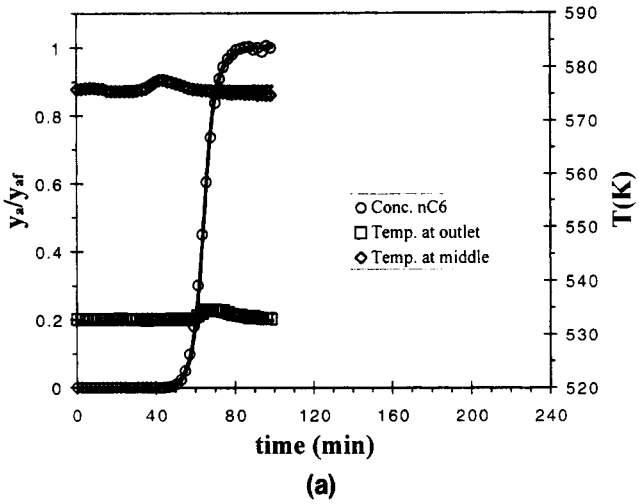

(a)

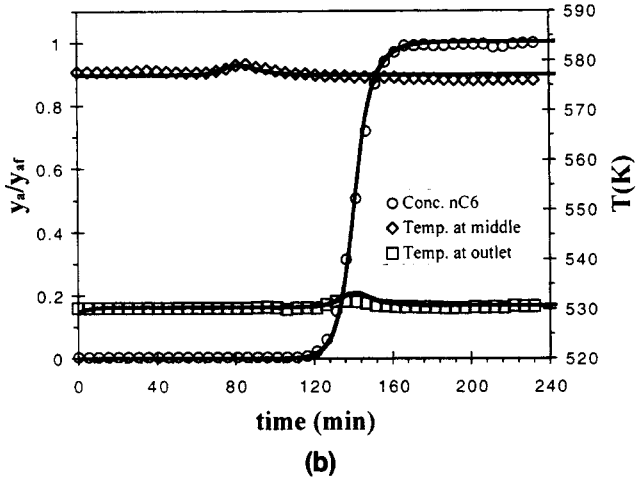

(b)

Figure 12. Effect of flow rate on experimental breakthrough curves of *n*-hexane, temperature histories at bed exit, and at 10 cm from bed inlet for adsorption of a mixture of N_2-nC_6 in pellets of zeolite 5A.

(a) $T_f = 513$ K; $y_{af} = 0.028$; $Q = 441$ mL/min (STP); $P_0 = 1$ atm. (b) $T_f = 513$ K; $y_{af} = 0.028$; $Q = 161$ mL/min (STP); $P_0 = 1$ atm. The lines are theoretical curves calculated according to the numerical solution of the dynamic model with parameters given in Table 6.

bar at 513 K. In the figure we also show the adsorption curve performed with a flow rate of 441 mL/min STP. If desorption was performed with a flow of inert gas similar to the total flow rate used in adsorption, the wash out of the column would practically double the time of adsorption. To reach a cycle time of the same order one has to double the purge flow rate, as can be clearly seen in Figure 13. This is expected for a system with a favorable isotherm, since in desorption concentration waves are dispersive.

Conclusions

A detailed study of adsorption and diffusion of *n*-hexane in commercial pellets of 5A zeolite was performed. The adsorption equilibrium was interpreted with a model of localized adsorption in a homogeneous surface, assuming that a

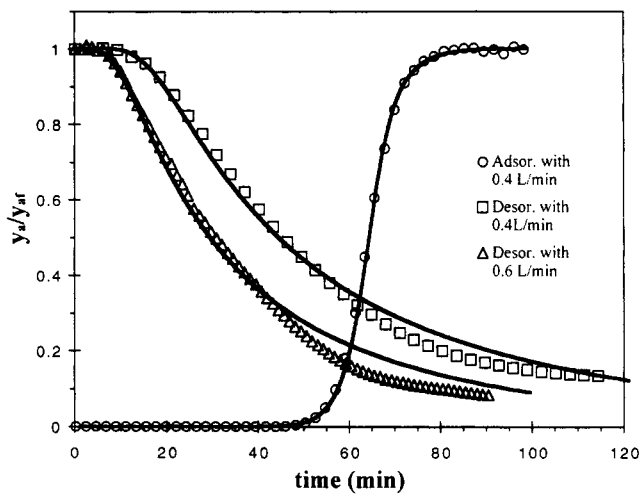

Figure 13. Effect of flow rate on desorption with nitrogen of a bed saturated with *n*-hexane ($y_{af} = 0.028$) at $T_f = 513$ K, $P_0 = 1$ atm, and $Q = 441$ mL/min (STP).

The lines are theoretical curves calculated according to the numerical solution of the dynamic model with parameters given in Table 6.

molecule when adsorbed occupies a certain number of active sites with no interaction between sorbed molecules. Mass transfer in the pellet was dominated at low loading of the adsorbent by macropore diffusion. This conclusion was confirmed by two independent experimental techniques, namely ZLC and gravimetry. The pore diffusivity of nC_6 in pellets of 5A zeolite ranges from 0.06 cm^2/s to 0.08 cm^2/s, when temperature changes from 473 K to 573 K in N_2 carrier gas; for the $He-nC_6$ system, the pore diffusivity in the same temperature range varies from 0.11 cm^2/s to 0.13 cm^2/s. The effect of temperature, partial-pressure of sorbate, and total flow rate was studied in a fixed bed where the influence of the favorable nature of the isotherm was dominant. A simple mathematical model with equilibrium and diffusivity parameters obtained in this work predicts with good accuracy all adsorption behavior.

The study provides the basic data needed for the design of a pressure swing adsorption cyclic process for the *n*/isoparaffins separation.

Acknowledgments

One of the authors (J. A. C. S.) acknowledges financial support from Junta Nacional de Investigação Científica e Tecnológica (Research fellowship; Praxis XXI/BD/3148/94).

Notation

a_c = specific area of column, m^{-1}
a_p = specific area of the pellet, m^{-1}
C_{pg} = heat capacity of gas, J/mol·K
C_{ps} = heat capacity of solid, J/kg·K
D_L = axial mass dispersion, m^2/s
F = total molar flux, mol/m^2·s
h_p = film heat-transfer coefficient, W/m^2·K
h_w = wall heat-transfer coefficient at the wall, W/m^2·K
K_{gl} = global mass-transfer coefficient, m/s
K_L = effective axial bed thermal conductivity, W/m·K
M_w = molecular mass of sorbate, g/mol

$\langle q \rangle$ = average adsorbed phase concentration, mol/kg
q_{af} = sorbed phase concentration at feed conditions, mol/kg
R = ideal gas flow constant, J/mol·K
r_c = crystal radius, m
R_p = pellet radius, m
t_{st} = stoichiometric time, s
y_a = mole fraction of sorbate in gas phase
$\langle y_a \rangle$ = average mole fraction of sorbate in the pellet pores
y_{af} = mole fraction of sorbate in gas phase at feed conditions
z = axial coordinate in bed, m
θ = fractional coverage of adsorbent, dimensionless
ϵ_b = bed porosity
ρ = total gas concentration, mol/m^3
τ_{dif} = time constant for diffusion in macropores ($= R_p^2/\epsilon_p \cdot D_p$), s
γ = ratio of macropore and micropore diffusion time constants, dimensionless

Literature Cited

Barrer, R. M., "Sorption in Porous Crystals: Equilibria and their Interpretation," *J. Chem. Tech. Biotechnol.*, **31**, 71 (1981).

Brandani, S., "Analytical Solution for ZLC Desorption Curves with bi-Porous Adsorbent Particles," *Chem. Eng. Sci.*, **51**, 3283 (1996).

Cavalcante, C. L., M. Eic, D. M. Ruthven, and M. L. Occeli, "Diffusion of n-Paraffins in Offretite-Erionite Type Zeolite," *Zeolites*, **15**, 293 (1995).

Crank, J., *The Mathematics of Diffusion*, Clarendon Press, Oxford (1975).

Doetsh, I. H., D. M. Ruthven, and K. F. Loughlin, "Sorption and Diffusion of n-Heptane in 5A Zeolite," *Can. J. Chem.*, **52**, 2717 (1974).

Dubinin, M. M., *Progress in Surface Science and Membrane Science*, Vol. 9, Academic Press, New York (1975).

Eberly, P. E., Jr., "Adsorption of Normal Paraffins in Erionite and 5A Molecular Sieve," *Ind. Eng. Chem. Prod. Res. Dev.*, **8**, 140 (1969).

Eic, M., and D. M. Ruthven, "A New Experimental Technique for Measurement of Intracrystalline Diffusivity," *Zeolites*, **8**, 41 (1988).

Grenier, Ph., V. Bourdin, L. M. Sun, and F. Meunier, "A Single Step Thermal Method to Measure Intracrystalline Mass Diffusion in Adsorbents," *AIChE J.*, **41**, 2047 (1995).

Holcombe, T. C., T. C. Sager, W. K. Volles, and A. Zarchy, "Isomerisation Process," U.S. Patent No. 4,929,799 (1990).

Hufton, R. J., and D. M. Ruthven, "Diffusion of Light Alkanes in Silicalite Studied by the Zero Length Column Method," *Ind. Eng. Chem. Res.*, **32**, 2379 (1993).

Karger, J., and D. M. Ruthven, *Diffusion in Zeolites and Other Microporous Solids*, Wiley, New York (1992).

Kiselev, A. V., "Vapor Adsorption on Zeolites Considered as Crystalline Specific Adsorbents," *ACS Symp. Ser.*, Vol. 102, R. F. Gould, ed., p. 37 (1971).

Langmuir, I., "The Adsorption of Gases on Plane Surfaces of Glass, Mica and Platinum," *J. Amer. Chem. Soc.*, **40**, 1361 (1918).

Martinez, G., and D. Basmadjian, "Towards a General Gas Adsorption Isotherm," *Chem. Eng. Sci.*, **51**, 1043 (1996).

Minkkinen, A., L. Mank, and S. Jullian, "Process for the Isomerization of C_5/C_6 Normal Paraffins with Recycling of Normal Paraffins," U.S. Patent No. 5,233,120 (1993).

Morbidelli, M., A. Servida, and G. Storti, "Carrà, Simulation of Multicomponent Adsorption Beds. Model Analysis and Numerical Solution," *Ind. Eng. Chem. Fundam.*, **21**, 123 (1982).

Nitta, T., T. Shigetomi, M. Kuro-Oka, and T. Katayama, "An Adsorption Isotherm of Multisite Occupancy Model for Homogeneous Surface," *J. Chem. Eng. Jpn.*, **17**, 39 (1984).

Rodrigues, A. E., "Modeling of Percolation Processes," *Percolation Processes: Theory and Applications*, A. E. Rodrigues and D. Tondeur, eds., Sijthoff & Noordhoff (now Kluwer), Alphen aan den Rijn, The Netherlands, p. 31 (1981).

Rodrigues, A. E., M. M. Dias, J. C. Lopes, N. Haisheng, V. G. Mata, and J. A. Silva, "Improved Efficiency of Adsorption Process," Final Rep., Contract JOUE-CT92-0076, AEA Technology, Harwell, U.K. (1996).

Ruckenstein, E., A. S. Vaidynathan, and G. R. Youngquist, "Sorption in Solids with Bidisperse Porous Structures," *Chem. Eng. Sci.*, **26**, 1305 (1971).

Ruthven, D. M., and K. F. Loughlin, "The Sorption and Diffusion of n-Butane in Linde 5A Molecular Sieve," *Chem. Eng. Sci.*, **26**, 1145 (1971).

Ruthven, D. M., and R. I. Derrah, "Sorption in Davison 5A Molecular Sieves," *Can. J. Chem. Eng.*, **50**, 743 (1972).

Ruthven, D. M., and K. F. Loughlin, "The Diffusional Resistance of Molecular Sieve Pellets," *Can. J. Chem. Eng.*, **28**, 550 (1972).

Ruthven, D. M., *Principles of Adsorption and Adsorption Process*, Wiley, New York (1984).

Ruthven, D. M., and B. K. Kaul, "Adsorption of n-Hexane and Intermediate Molecular Weight Aromatic Hydrocarbons on LaY Zeolite," *Ind. Eng. Chem. Res.*, **35**, 2060 (1996).

Silva, J. A., and A. E. Rodrigues, "Analysis of ZLC Technique for Diffusivity Measurements in Bidisperse Porous Adsorbent Pellets," *Gas. Sep. Purif.*, **10**(4), 207 (1996).

Silva, J. A., and A. E. Rodrigues, "Sorption and Diffusion on n-Pentane in Pellets of 5A Zeolite," *Ind. Eng. Chem. Res.*, **36**, 493 (1997a).

Silva, J. A., and A. E. Rodrigues, "Fixed Bed Adsorption of n/Iso-Pentane Mixtures in Pellets of 5A Zeolite," *Ind. Eng. Chem. Res.* (1997b).

Sircar, S., "Influence of Adsorbate Size and Adsorbent Heterogeneity on IAST," *AIChE J.*, **41**, 1135 (1995).

Symoniak, M. F., "Upgrade Naphtha to ... Fuels and Feedstocks," *Hydroc. Process.*, 110 (May, 1980).

Talu, O., and A. L. Myers, "Rigorous Thermodynamic Treatment of Gas Adsorption," *AIChE J.*, **34**, 1893 (1988).

Villadsen, J. V., and M. L. Michelsen, *Solution of Differential Equation Models by Polynomial Approximation*, Prentice Hall, Englewood Cliffs, NJ (1978).

Yang, R. T., *Gas Separation by Adsorption Process*, Butterworth, Stoneham, MA (1987).

Youngquist, G. R., J. L. Allen, and J. Eisenberg, "Adsorption of Hydrocarbons by Synthetic Zeolites," *Ind. Eng. Chem. Prod. Res. Dev.*, **10**(3), 308 (1971).

Zuech, J. L., A. L. Hines, and E. D. Sloan, "Methane Adsorption on 5A Molecular Sieve in the Pressure Range 4 to 690 kPa," *Ind. Eng. Chem. Process Des. Dev.*, **22**, 172 (1983).

Manuscript received Apr. 1, 1997, and revision received June 9, 1997.